Acta Crystallographica Section F
Structural Biology and Crystallization Communications
ISSN 1744-3091

Crystallization of the FaeE chaperone of *Escherichia coli* F4 fimbriae

Inge Van Molle,* Lieven Buts, Fanny Coppens, Liu Qiang,‡ Lode Wyns, Remy Loris, Julie Bouckaert and Henri De Greve

Laboratorium voor Ultrastructuur, Vlaams Interuniversitair Instituut voor Biotechnologie, Vrije Universiteit Brussel, Pleinlaan 2, 1050 Brussel, Belgium

‡ Current address: Research Center of Centre Hospitalier de l'Université de Montreal, Hotel-Dieu, Pavillon Masson 3850, Rue Saint-Urbain, Montreal H2W 1T8, Canada.

Correspondence e-mail: ivmolle@vub.ac.be

Received 21 January 2005
Accepted 16 March 2005
Online 1 April 2005

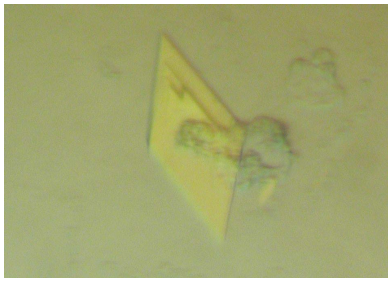

F4 (formerly K88) fimbriae from enterotoxigenic *Escherichia coli* are assembled *via* the FaeE/FaeD chaperone/usher pathway. The chaperone FaeE crystallizes in three crystal forms, all belonging to space group *C*2. Crystals of form 1 diffract to 2.3 Å and have unit-cell parameters $a = 195.7$, $b = 78.5$, $c = 184.6$ Å, $\beta = 102.2^\circ$. X-ray data for crystal form 2 were collected to 2.7 Å using an SeMet variant of FaeE. The crystals have unit-cell parameters $a = 136.4$, $b = 75.7$, $c = 69.4$ Å, $\beta = 92.8^\circ$. Crystals of form 3 were formed in a solution containing the FaeE–FaeG complex and diffract to 2.8 Å. Unit-cell parameters are $a = 109.7$, $b = 78.6$, $c = 87.8$ Å, $\beta = 96.4^\circ$.

1. Introduction

Early steps in bacterial pathogenesis involve the attachment of the bacteria to the host cell, often mediated by recognition of carbohydrate moieties on cell-surface receptors by fimbrial adhesins (Hultgren *et al.*, 1996). Assembly of fimbriae or pili on the surface of Gram-negative bacteria in many cases occurs *via* the chaperone/usher pathway (Thanassi *et al.*, 1998). The crystal structures of the fimbrial chaperones PapD, FimC and SfaeE show that they all share the same overall boomerang-shaped structure containing two immunoglobulin-like domains (Holmgren *et al.*, 1992; Pellecchia *et al.*, 1998; Knight *et al.*, 2002). The structures of the FimC–FimH and PapD–PapK complexes revealed that the fimbrial subunits also have an immunoglobulin-like fold, but lack the seventh β-strand. The absence of this strand results in a deep groove, exposing the hydrophobic core of the subunit to the surface (Choudhury *et al.*, 1999; Sauer *et al.*, 1999). Fimbrial chaperones bind the subunits as they are translocated to the periplasm by the Sec machinery and protect them from degradation, aggregation and premature fibre formation by capping their assembly surfaces. In a mechanism called donor-strand complementation, the chaperone's G_1 β-strand is inserted into the groove on the surface of the subunit (Kuehn *et al.*, 1991, 1993; Choudhury *et al.*, 1999; Sauer *et al.*, 1999). The chaperone thereby also helps the subunit to fold correctly (Barnhart *et al.*, 2000; Sauer *et al.*, 2000). During pilus biogenesis, the conserved N-terminal extension of one subunit replaces the chaperone's G_1 β-strand from its neighbouring subunit in a mechanism called donor-strand exchange (Choudhury *et al.*, 1999; Sauer *et al.*, 1999).

F4 fimbriae are expressed by enterotoxigenic *Escherichia coli* strains that cause diarrhoea in neonatal or recently weaned piglets (de Graaf & Mooi, 1986). In contrast to type 1 and P pili, F4 pili are not built up of a helical rod consisting of major subunits followed by a fibrillum of minor subunits and a tip adhesin. Rather, F4 pili are thin flexible structures consisting mainly of the major subunit FaeG, which also contains the adhesive properties (Gaastra & de Graaf, 1982). Mol and coworkers revealed that the F4 chaperone FaeE is a homodimer and forms heterotrimeric complexes with the F4 fimbrial subunits (Mol *et al.*, 1994, 1995, 1996). These results cannot readily be explained in the light of current knowledge on the donor-strand complementation/donor-strand exchange mechanism. So far, only 1:1

chaperone–subunit complexes have been identified. Chaperone dimerization has been observed for PapD and SfaE. In both cases, the subunit-binding interface of the chaperone is involved in dimerization (Hung *et al.*, 1999; Knight *et al.*, 2002). Therefore, further research into F4 fimbrial biogenesis is necessary to clarify the molecular and structural basis of the F4 chaperone dimerization and the F4 chaperone–subunit interactions. Here, we report the crystallization of the FaeE chaperone.

2. Materials and methods

2.1. Expression and purification

2.1.1. Co-expression and purification of the FaeE–FaeG complex. The fragment of the F4 operon containing the *faeE*, *faeF* and *faeG* genes was amplified from the F4ad$^+$ *E. coli* C1360-79 genome using PCR with the forward primer K88-4 (5′-AGT AAG CGT AAC GCA GTA ACG ACG TTT TTC-3′, based on accession No. X56003) and the reverse primer K88-2 (5′-GGG GTC GAC CTA GTA ATA AGT AAT TGC TAC GTT CAG-3′, based on accession No. V00292). The fragment was inserted into plasmid pHD40 between a blunted *Nco*I and a *Sal*I restriction site. This vector is a derivative of a pBAD vector in which the araBAD promotor was replaced by the T7 promotor. The FaeF gene was cut out using *Bsp*EI and the plasmid was self-ligated using Ready-To-Go T4 DNA ligase (Amersham Biosciences). After transformation in *E. coli* K514, colonies were grown on Luria Broth–agar plates containing 100 µg ml^{-1} ampicillin. DNA-sequence analyses on the transformants were performed using an ABI PRISM 3100 Genetic Analyzer (Applied Biosciences). The plasmid used in further experiments was designed pHD147 and transformed in *E. coli* C43 (DE3) (Miroux & Walker, 1996). An overnight culture of *E. coli* C43 (DE3) (pHD147) grown at 310 K in Luria Broth (LB) medium supplemented with 100 µg ml^{-1} ampicillin was diluted 20 times in LB medium and incubated at 310 K. When OD_{600} reached 0.7, gene expression was induced with 1 m*M* isopropyl-β-D-thiogalactopyranoside (IPTG). Cells were harvested 3 h after induction by centrifugation (10 min, 4500 rev min^{-1}; Beckman JLA8100 rotor) and the periplasmic fraction was extracted by osmotic shock. In brief, pellets were resuspended in 20 m*M* *N*-Tris(hydroxymethyl)methyl-2-aminoethanesulfonic acid (TES) pH 7.0, 30% sucrose and 2.5 m*M* ethylenediaminetetraacetic acid (EDTA) and incubated on ice for 1 h. The suspension was centrifuged for 20 min at 10 000 rev min^{-1} using a Beckman JA20 rotor. The pellet was resuspended in 20 m*M* TES pH 7.0 and incubated on ice for 30 min. After centrifugation at 10 000 rev min^{-1} for 20 min, the supernatants containing the periplasmic fraction were collected. The periplasmic extract was immediately loaded onto a Poros 50HQ anion-exchange column (Applied Biosystems) equilibrated in 20 m*M* TES buffer pH 7.0. The column was eluted using a linear gradient to 20 m*M* TES pH 7.0, 1 *M* NaCl. Fractions containing the FaeE–FaeG complex were pooled, concentrated using Vivaspin 10 kDa cutoff concentrators (Vivascience) and loaded onto a Superdex 75 HR1030 gel-filtration column (Amersham Pharmacia) equilibrated in 20 m*M* TES pH 7.0, 150 m*M* NaCl.

2.1.2. Expression and purification of FaeE. The *faeG* gene was deleted from pHD147 using *Sal*I and *Bst*EII restriction followed by ligation. The resulting plasmid pHD163 was transformed in *E. coli* C43 (DE3). FaeE was expressed as described for FaeE–FaeG. The periplasmic extract was loaded onto a Poros 50HS cation-exchange column (Applied Biosystems) in 20 m*M* TES pH 7.0. The column was eluted using a linear gradient to 20 m*M* TES pH 7.0, 1 *M* NaCl. Fractions containing the FaeE protein were pooled, concentrated using Vivaspin 10 kDa cutoff concentrators (Vivascience) and loaded onto a Superdex 75HR1030 gel-filtration column (Amersham Pharmacia) equilibrated in 20 m*M* TES pH 7.0, 150 m*M* NaCl.

2.1.3. Expression and purification of FaeE$_{SeMet}$. In order to purify the selenomethionine variant of FaeE (FaeE$_{SeMet}$), pHD163 was transformed in the methionine auxotroph *E. coli* B834 (DE3) (Leahy *et al.*, 1992). *E. coli* B834(DE3) (pHD163) was grown overnight at 310 K in minimal medium supplemented with 40 µg ml^{-1} of all amino acids, 2 µg ml^{-1} biotin, 2 µg ml^{-1} thiamine, 0.2% glucose, 2 m*M* $MgSO_4$ and 100 µg ml^{-1} ampicillin. This culture was diluted 20 times in minimal medium supplemented with 40 µg ml^{-1} of all amino acids except methionine, 40 µg ml^{-1} selenomethionine, 2 µg ml^{-1} biotin, 2 µg ml^{-1} thiamine, 0.2% glucose, 2 m*M* $MgSO_4$ and incubated at 310 K. When OD_{600} reached 0.7, gene expression was induced with 1 m*M* IPTG. Cells were harvested 3 h after induction by centrifuga-

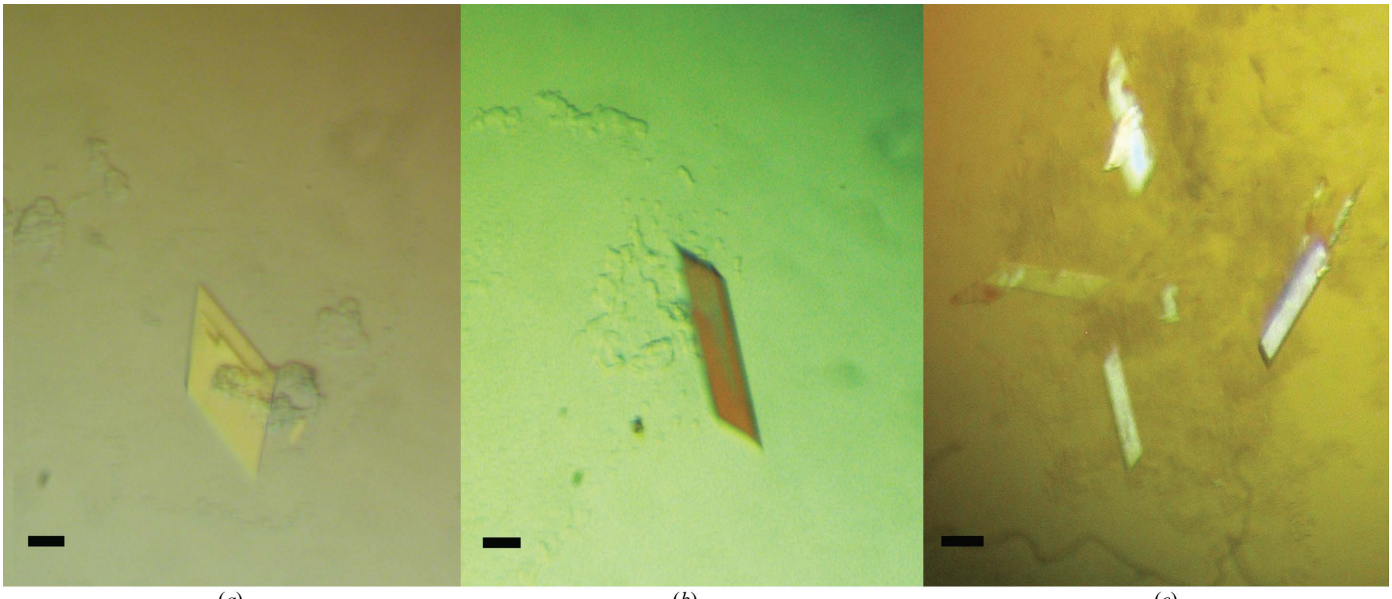

(*a*) (*b*) (*c*)

Figure 1
Crystals of FaeE. (*a*) FaeE crystal form 1, grown in 0.1 *M* Tris pH 8.5, 50% MPD. (*b*) FaeE crystal form 2, grown in 0.1 *M* HEPES pH 7.5, 50% MPD, 0.05 *M* $NH_4H_2PO_4$. (*c*) FaeE crystal form 3, grown in 0.1 *M* Tris pH 8.5, 50% MPD, 0.1 *M* $NH_4H_2PO_4$ from drops initially containing the FaeE–FaeG complex. The black bars indicate 0.1 mm.

tion (10 min, 4500 rev min^{-1}, Beckman JLA 8100) and the periplasmic fraction was extracted by osmotic shock (see §2.1.1). Purification of FaE$_{SeMet}$ was identical to that of FaeE.

2.2. Crystallization and X-ray analysis

Prior to crystallization, the proteins were concentrated using the same Vivaspin concentrators as above (to 15 mg ml^{-1} for FaeE–FaeG and to 35 mg ml^{-1} for FaeE). The particle distribution of the protein samples was analysed using dynamic light scattering (DLS; RiNA, Netzwerk RNA Technologien). Crystallizations were performed using the hanging-drop vapour-diffusion method at 293 K. Crystallization drops containing 1 µl protein solution in 20 m*M* TES pH 7.0, 150 m*M* NaCl and 1 µl precipitant solution were equilibrated against 500 µl precipitant solution. Crystallization conditions were screened using the Crystal Screen and Crystal Screen 2 kits (Hampton Research). Positive conditions were further optimized. Crystallization conditions for FaE$_{SeMet}$ were based on the conditions established for FaeE.

X-ray data for FaeE were collected at ESRF beamline ID14-1 (Grenoble, France) and DESY/EMBL beamline BW7A (Hamburg, Germany). Data for FaE$_{SeMet}$ were collected at the absorption-edge, inflection-point and high-energy remote wavelengths as determined by a fluorescence scan for selenium. Data were indexed and processed using *DENZO* and *SCALEPACK* from the *HKL* suite (Otwinowski & Minor, 1997). *TRUNCATE* and *MATTHEWS_COEFF* from the *CCP*4 suite (Collaborative Computational Project, Number 4, 1994) were used to obtain structure-factor amplitudes and calculate solvent contents, respectively. Preliminary phases from the MAD data were calculated at the EMBL facility using the experimental *Auto-Rickshaw* automated crystal structure determination platform (Panjikar *et al.*, 2005).

2.3. SDS–PAGE analysis

Crystals were picked from the hanging drop, washed in precipitant solution and dissolved in H_2O. The remaining solution was diluted fivefold in H_2O. Samples were heated at 373 K for 5 min prior to analysis on 12.5% SDS–polyacrylamide gels.

3. Results and discussion

FaeE–FaeG, FaeE and FaE$_{SeMet}$ showed high expression levels, were purified to a high degree and had a monodisperse particle distribution according to DLS measurements. Screening for FaeE crystallization conditions using Crystal Screen 2 (35 mg ml^{-1} FaeE) resulted in crystal formation in condition No. 43 [0.1 *M* Tris pH 8.5, 50%(*v*/*v*) 2-methyl-2,4-pentanediol (MPD), 0.2 *M* $NH_4H_2PO_4$]. Lowering the FaeE concentration to 20 mg ml^{-1} and changing the buffer to 0.1 *M* HEPES pH 7.5 resulted in larger crystals. Crystals were grown in a range of $NH_4H_2PO_4$ concentrations (0.5–0.2 *M*) or in the absence of $NH_4H_2PO_4$. Mother liquor containing 50% MPD was used as the cryoprotectant. Crystals were flash-frozen directly in the cryostream. FaeE showed two crystal forms (Figs. 1*a* and 1*b*), which occurred using the same condition and even in the same drop. Both crystal forms 1 and 2 belong to space group *C*2 and diffracted to 2.3 Å (Fig. 2*a*) and 4 Å (data not shown), respectively. Single crystals of FaE$_{SeMet}$ (using a protein concentration of 25 mg ml^{-1}) were obtained using one of the conditions established for FaeE. An X-ray data set was collected for a FaE$_{SeMet}$ crystal to 2.7 Å resolution at three wavelengths (Fig. 2*b*). This crystal showed the same unit-cell parameters as FaeE crystal form 2. Data-collection statistics are summarized in Table 1.

Preliminary phases from the MAD data obtained using the *Auto-Rickshaw* program at the EMBL facility revealed eight Se peaks in the asymmetric unit of the FaE$_{SeMet}$ crystals. Four selenomethionine residues are present in FaeE, indicating that the asymmetric unit contains two FaeE molecules. A Matthews coefficient calculation shows that this asymmetric unit has 65% solvent content (FaE$_{SeMet}$

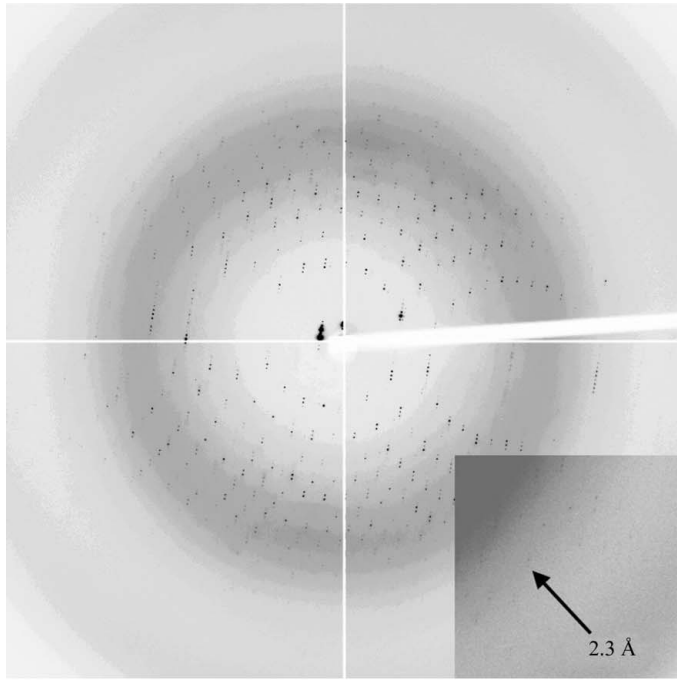

(*a*)

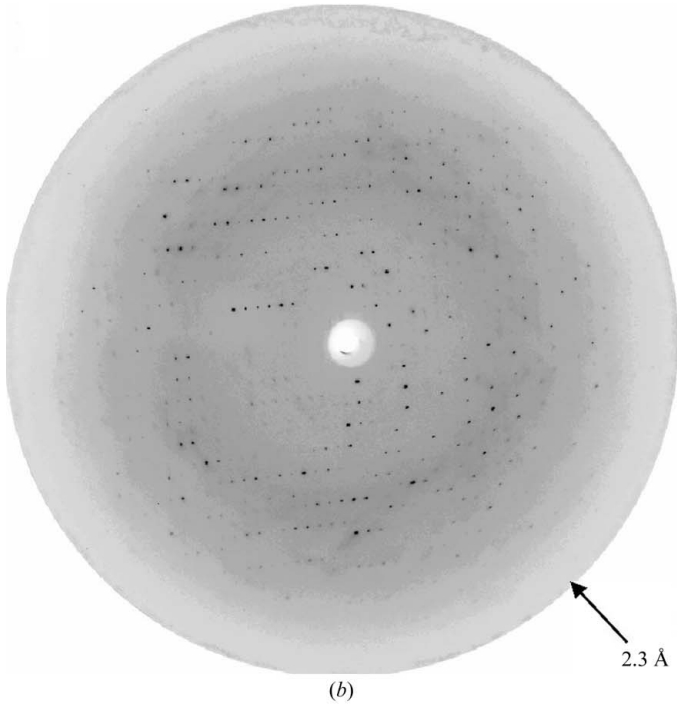

(*b*)

Figure 2
Diffraction patterns of form 1 and 2 FaeE crystals. (*a*) FaeE crystal form 1 exposed for 5 s on ESRF beamline ID14-1 (Grenoble, France) at a wavelength of 0.933 Å and with a detector distance of 215 mm. The arrowhead indicates a resolution of 2.3 Å. (*b*) FaeE crystal form 2 (FaE$_{SeMet}$ crystal) exposed for 50 s on the EMBL BW7A beamline at the DESY synchrotron (Hamburg, Germany) at a wavelength of 0.9789 Å and with a detector distance of 201 mm.

Table 1
Data-collection statistics and crystal parameters for the different crystal forms of FaeE.

Values in parentheses are for the highest resolution shells.

		FaeE crystal form 2 (data collected from $FaeE_{SeMet}$ crystal)			
	FaeE crystal form 1	Absorption edge	Inflection point	High-energy remote	FaeE crystal form 3
Wavelength (Å)	0.933	0.9789	0.9796	0.9364	0.9364
Resolution range (Å)	49.8–2.3 (2.4–2.3)	39.0–2.7 (2.8–2.7)	39.0–2.7 (2.8–2.7)	33.0–2.7 (2.8–2.7)	39.3–2.8 (2.9–2.8)
Total reflections	639018	145440	140236	149032	111565
Unique reflections	122618 (11697)	19280 (1903)	19271 (1920)	19389 (1890)	18291 (1794)
Redundancy	5.2 (4.0)	7.5 (7.4)	7.3 (7.2)	7.7 (7.4)	6.1 (6.2)
Mosaicity (°)	0.3	0.7	0.7	0.7	1.4
$\langle I/\sigma(I)\rangle$	14.56 (3.7)	19.5 (5.4)	19.3 (5.3)	23.97 (4.9)	14.91 (7.0)
Completeness (%)	99.5 (95.6)	98.0 (97.1)	98.0 (98.2)	98.6 (96.4)	99.8 (100.0)
R_{merge} (%)	8.3 (39.0)	7.1 (32.9)	5.7 (29.9)	5.3 (40.4)	12.2 (30.2)
R_{anom} (%)		3.7 (10.0)	1.7 (9.9)	2.6 (13.8)	
Space group	*C*2	*C*2			*C*2
Unit-cell parameters					
a (Å)	195.7	136.4			109.7
b (Å)	78.5	75.7			78.6
c (Å)	184.6	69.4			87.8
β (°)	102.2	92.8			96.4
Beamline	ID14-1	BW7A			BW7A

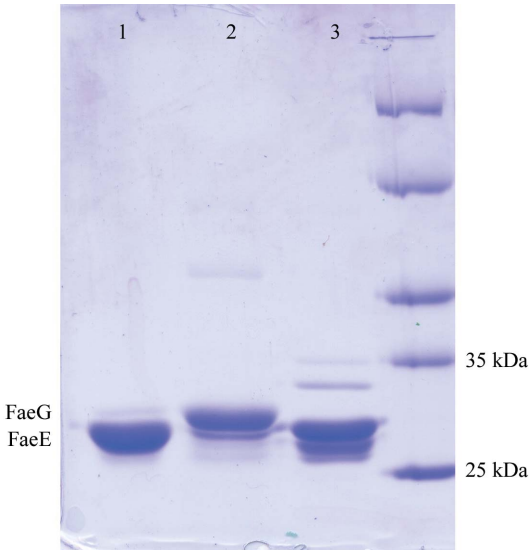

Figure 3
SDS–PAGE analysis of the FaeE–FaeG crystallization. Lane 1, crystals grown in solutions initially containing the FaeE–FaeG complex, showing clearly that only FaeE is present. Lane 2, liquid remaining in the hanging drop after removal of the crystals, showing an excess of FaeG. Lane 3, control sample of purified FaeE.

molecular weight, 25.0 kDa; Matthews coefficient, 3.6 $Å^3$ Da^{-1}). The Matthews coefficient for FaeE crystal form 1 could be in the range 1.7 $Å^3$ Da^{-1} (16 molecules per asymmetric unit, 29% solvent content) to 5.6 $Å^3$ Da^{-1} (five molecules per asymmetric unit, 77% solvent content) (molecular weight of FaeE, 24.7 kDa). Given the proportion of the unit-cell volumes of crystal forms 1 and 2 (3.8), the asymmetric unit of crystal form 1 is likely to contain at least eight molecules (Matthews coefficient 3.5 $Å^3$ Da^{-1}, 65% solvent content).

Crystal form 3 (Fig. 1*c*) was obtained in solutions containing the FaeE–FaeG chaperone–adhesin complex equilibrated against a precipitant solution of 0.1 *M* Tris pH 8.5, 50%(*v*/*v*) 2-methyl-2,4-pentanediol (MPD) and a range of $NH_4H_2PO_4$ concentrations (0.5–0.2 *M*). SDS–PAGE revealed that these crystals did not contain the FaeE–FaeG complex but only the FaeE chaperone (Fig. 3). Under the conditions used only FaeE crystallizes, while FaeG precipitates, probably owing to self-polymerization. X-ray data from the crystals were collected to 2.8 Å (Table 1). The Matthews coefficient for this crystal form could be in the range 3.8 $Å^3$ Da^{-1} (two molecules per asymmetric unit, 67.4% solvent content) to 1.9 $Å^3$ Da^{-1} (four molecules per asymmetric unit, 34.9% solvent content).

The authors thank S. Panjikar for his excellent assistance by introducing us to the experimental *Auto-Rickshaw* automated crystal structure determination. JB is a postdoctoral fellow of the Fonds voor Wetenschappelijk Onderzoek-Vlaanderen (FWO-Vlaanderen). Financial support for this project was provided by the Research Council of the Vrije Universiteit Brussel (OZR846, OZR727 and OZR728) and the FWO-Vlaanderen (FWOAL241). The authors acknowledge the use of the EMBL beamline BW7A at the DESY synchrotron (Hamburg, Germay) and the use of the ESRF beamline ID14-1 (Grenoble, France).

References

Barnhart, M. M., Pinkner, J. S., Soto, G. E., Sauer, F. G., Langermann, S., Waksman, G., Frieden, C. & Hultgren, S. J. (2000). *Proc. Natl Acad. Sci. USA*, **97**, 7709–7714.
Choudhury, D., Thompson, A., Stojanoff, V., Langermann, S., Pinkner, J., Hultgren, S. J. & Knight, S. D. (1999). *Science*, **285**, 1061–1066.
Collaborative Computational Project, Number 4 (1994). *Acta Cryst.* D**50**, 760–763.
Gaastra, W. & de Graaf, F. K. (1982). *Microbiol. Rev.* **46**, 129–161.
Graaf, F. K. de & Mooi, F. R. (1986). *Adv. Microb. Physiol.* **28**, 65–143.
Holmgren, A., Kuehn, M. J., Branden, C. I. & Hultgren, S. J. (1992). *EMBO J.* **11**, 1617–1622.
Hultgren, S. J., Jones, C. H. & Normark, S. (1996). In *Escherichia coli and Salmonella: Cellular and Molecular Biology*, edited by F. C. Neidhardt. Washington DC: ASM Press.
Hung, D. L., Pinkner, J. S., Knight, S. D. & Hultgren, S. J. (1999). *Proc. Natl Acad. Sci. USA*, **96**, 8178–8183.
Knight, S. D., Choudhury, D., Hultgren, S., Pinkner, J., Stojanoff, V. & Thompson, A. (2002). *Acta Cryst.* D**58**, 1016–1022.
Kuehn, M. J., Normark, S. & Hultgren, S. J. (1991). *Proc. Natl Acad. Sci. USA*, **88**, 10586–10590.
Kuehn, M. J., Ogg, D. J., Kihlberg, J., Slonim, L. N., Flemmer, K., Bergfors, T. & Hultgren, S. J. (1993). *Science*, **262**, 1234–1241.
Leahy, D. J., Hendrickson, W. A., Aukhil, I. & Erickson, H. P. (1992). *Science*, **258**, 987–991.
Miroux, B. & Walker, J. E. (1996). *J. Mol. Biol.* **260**, 289–298.
Mol, O., Oud, R. P., de Graaf, F. K. & Oudega, B. (1995). *Microb. Pathog.* **18**, 115–128.
Mol, O., Oudhuis, W. C., Fokkema, H. & Oudega, B. (1996). *Mol. Microbiol.* **22**, 379–388.

Mol, O., Visschers, R. W., de Graaf, F. K. & Oudega, B. (1994). *Mol. Microbiol.* **11**, 391–402.
Otwinowski, Z. & Minor, W. (1997). *Methods Enzymol.* **276**, 307–326.
Panjikar, S., Parthasarathy, V., Lamzin, V. S., Weiss, M. S. & Tucker, P. A. (2005). *Acta Cryst.* D**61**, 449–457.
Pellecchia, M., Guntert, P., Glockshuber, R. & Wuthrich, K. (1998). *Nature Struct. Biol.* **5**, 885–890.
Sauer, F. G., Barnhart, M., Choudhury, D., Knight, S. D., Waksman, G. & Hultgren, S. J. (2000). *Curr. Opin. Struct. Biol.* **10**, 548–556.
Sauer, F. G., Futterer, K., Pinkner, J. S., Dodson, K. W., Hultgren, S. J. & Waksman, G. (1999). *Science*, **285**, 1058–1061.
Thanassi, D. G., Saulino, E. T. & Hultgren, S. J. (1998). *Curr. Opin. Microbiol.* **1**, 223–231.